A Generalized Theory of an Electrolyte-Insulator-Semiconductor Field-Effect Transistor

CLIFFORD D. FUNG, MEMBER, IEEE, PETER W. CHEUNG, MEMBER, IEEE, AND WEN H. KO, FELLOW, IEEE

Abstract—A model of surface ionization and complexation of surface hydroxyl groups on the gate insulator surface is adapted in conjunction with electronic device physics to arrive at a generalized theory for the current–voltage characteristics of an electrolyte-insulator-semiconductor field-effect transistor (EISFET) in electrolyte solutions. EISFET's that employ thermally grown silicon dioxide were tested in simple electrolytes that contain Na^+, K^+, and Li^+ ions titrated in a pH range from 2 to 9. Experimental results show good agreement with the theory. The model successfully explains pH sensitivity, as well as the ion interference effect, of the EISFET working as a pH sensor. From this model, it is concluded that, among all the electrolyte parameters associated with an EISFET, the surface site density of the hydroxyl groups N_s and the separation of surface ionization constants ΔpK are the primary factors to consider when employing EISFET's as pH sensors. For high sensitivity and good selectivity, large N_s and small ΔpK values are required.

I. INTRODUCTION

IN PAST YEARS, much work has been done to demonstrate the feasibility of using ion-sensitive field-effect transistors (ISFET's) [1], [2] for measuring pH and other ions in the electrolyte. For the category of ISFET's that use an ion-selective membrane on top of the gate insulator film, the device response can be satisfactorily explained by the well-established theory of ion-selective electrodes, whereas the principle of ISFET's that employ only an inorganic insulator film without an ion-selective membrane is not well understood.

When Bergveld first introduced the ISFET [3], [4] the device was operated without a reference electrode. However, later work by other investigators [5], [6] indicates that proper operation of the ISFET requires a reference electrode to establish the electrolyte potential with respect to the semiconductor substrate. This type of ISFET, which is operated with a reference electrode and consists of a gate structure of electrolyte–insulator–semiconductor (EIS) interfaces, will be referred to as the electrolyte-insulator-semiconductor field-effect transistor (EISFET) [7].

Early attempts to model the response of EISFET's were based upon an empirical approach that combines the glass-electrode potential with the device physics of a metal-oxide-semiconductor field-effect transistor (MOSFET) [8],

[9] and were not able to account for many of the experimental observations on the output sensitivity to hydrogen ions and the output selectivity for hydrogen ions over the other ions in the solution. In particular, it failed to predict an often observed non-Nernstian response with pH. Different mechanisms were suggested to identify the origin of the EISFET response in solutions. The influence on the interface state density at the insulator–semiconductor interface was once speculated to be responsible for the operation of EISFET's [10]. However, at a later time, experimental results indicated that it was unlikely for such a phenomenon to cause the response of an EISFET [11], [12]. The behavior of EISFET's is primarily attributed to an interfacial potential developed at the insulator–electrolyte interface [12], [13]. An experiment was designed to study the effect on EISFET response by modifying the EISFET at the surface of its gate insulator during the fabrication process [13], [14]. In the experiment, the composite gate insulator layer consisting of silicon nitride on silicon dioxide was oxidized using wet oxygen at 1050°C to convert the silicon nitride surface into a silicon oxide layer approximately 150 Å in thickness. The response of the surface-oxidized nitride-gate EISFET degraded to that of a silicon-dioxide-gate EISFET, with lower pH sensitivity and decreased selectivity. When the oxidized surface layer was removed, the response of the device recovered to that of the nitride-gate EISFET. This experiment established the surface-dominant behavior of the device. Siu *et al.* [15] used the site-binding model by Yates *et al.* [16] to describe the ionic absorption processes at the electrolyte–SiO_2 interface and to examine the flat-band voltage of the electrolyte–SiO_2–Si system in response to pH. A similar approach was taken by Fung *et al.* [7], [14] and Bousse *et al.* [17] to study the characteristics of EISFET's and the operation of chemically sensitive field-effect sensors, respectively. From this point of view, the EISFET can be regarded as a transistor that measures the phenomena occurring at the insulator–electrolyte interface through a field effect.

Based on the concept originally presented in [7], this paper describes a full theoretical development of a generalized model with a detailed discussion of experimental and theoretical results. A model of surface ionization and complexation by Yates *et al.* [16] and Davis *et al.* [18] is merged with the physics of a MOSFET to arrive at this generalized theory for the EISFET. The theory is general in the sense that 1) it can explain quantitatively the EIS-

FET response to hydrogen ions, as well as other ions present in electrolyte solutions; 2) the derivation of the EIS-FET current–voltage characteristics relies on the solution of a general set of equations that describe the EIS system. (These equations can be readily modified or extended for a different or more sophisticated system.) Based on this theory, a detailed discussion of the EISFET's electrochemical parameters with regard to the device's performance as a pH sensor is then presented.
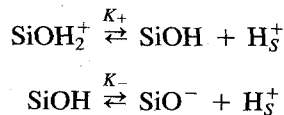
II. THEORETICAL MODEL OF DEVICE CHARACTERISTICS

In this section the surface interaction at the electrolyte–insulator interface will be described first, followed by a study of the charge and potential distributions across an ideal EIS structure. The drain current–voltage characteristics of an EISFET is then developed based on conventional MOSFET theory.

A. Surface Interaction and Ideal EIS Structure

At a blocked insulator–electrolyte interface involved in an EISFET, ions are distributed only between the solution and the surface of the solid with neither electron nor ion exchange across the boundary of the two phases. The electrical double layer of oxide suspensions has been a subject extensively studied by colloid and surface scientists. In explaining interactions of electrolyte ions with oxide surfaces, some researchers have emphasized the structural and the physical aspect of the distribution of solutes. Others have stressed the specific chemical interactions of solutes with oxide surfaces and solution. However, no comprehensive model existed for simultaneously estimating adsorption density, surface charge, stoichiometry of surface reactions, and diffuse layer potentials at the oxide–electrolyte interface until the work of Yates et al. [16] and Davies et al. [18] appeared. Their work resulted in major improvements in the double-layer model by including the formation of surface complexes in addition to simple ionization of surface hydroxyl groups by interactions with hydrogen and hydroxyl ions. The model is reasonably complete in that both the physical interaction in controlling the distribution of ions and the chemical interaction of the ions with the oxide simultaneously considered. Their model can be readily generalized to account for other blocked insulator–electrolyte interfaces with similar surface sites.

For insulators containing hydroxyl groups, using silicon dioxide as an example, the chemical reaction at the interface can be described as follows [18]:
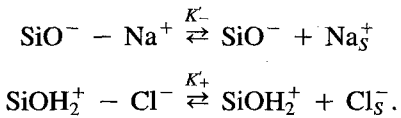
$$SiOH_2^+ \overset{K_+}{\rightleftharpoons} SiOH + H_S^+$$

$$SiOH \overset{K_-}{\rightleftharpoons} SiO^- + H_S^+$$

The amphoteric dissociation constants for the above equilibria are given by

$$K_+ = \frac{[SiOH][H^+]_S}{[SiOH_2^+]} \qquad (1)$$

$$K_- = \frac{[SiO^-][H^+]_S}{[SiOH]} \qquad (2)$$

Since H^+ and OH^- are the predominant ions in determining the charges and, in turn, the potentials at the electrical double layer, they are referred to as the potential-determining ions for this interface. The other ions in the electrolyte are referred to as supporting-electrolyte ions or, simply, electrolyte ions.

In addition to the amphoteric dissociation, the supporting electrolyte can also form ion pairs with the charged surface sites. This process will be referred to as surface complexation and is illustrated below using NaCl as a typical univalent supporting electrolyte.

$$SiO^- - Na^+ \overset{K'_-}{\rightleftharpoons} SiO^- + Na_S^+$$

$$SiOH_2^+ - Cl^- \overset{K'_+}{\rightleftharpoons} SiOH_2^+ + Cl_S^-.$$

The equilibrium constants can again be written as

$$K'_- = \frac{[SiO^-][Na^+]_S}{[SiO^- - Na^+]} \qquad (3)$$

$$K'_+ = \frac{[SiOH_2^+][Cl^-]_S}{[SiOH_2^+ - Cl^-]}. \qquad (4)$$

While the surface complexation depends on the existing SiO^- and $SiOH_2^+$ sites, the formation of surface complexes also readjusts the acid–base equilibrium and affects the surface charge.

The charge density and electrostatic potential at different locations of the electrical double layer at the interface are shown in Fig. 1, where the outer Helmholtz plane (OHP) is the locus of the centers of the hyrated ions with the closest approach to the solid, and the inner Helmholtz plane (IHP) is the plane of the adsorbed ions which form pairs with the charged surface sites [18]. According to the Boltzmann distribution, the concentration of an ion species X at a location i in the electrical double layer $[X]_i$ as related to the bulk concentration $[X]$ is given by

$$[X]_i = [X] \exp [-q\psi_i/kT].$$

Therefore, (1) may be rewritten as

$$K_+ = \frac{[SiOH][H^+]}{[SiOH_2^+]} \exp (-q\psi_0/kT) \qquad (5)$$

where $[H^+]$ is the bulk concentration of H^+ and $[H^+]_S = [H^+] \exp (-q\psi_0/kT)$ is used.

Likewise, (2) is rewritten as

$$K_- = \frac{[SiO^-][H^+]}{[SiOH]} \exp (-q\psi_0/kT). \qquad (6)$$

Since $[Na^+]_S = [Na^+] \exp (-q\psi_\beta/kT)$ and $[Cl^-]_S = [Cl^-] \exp (q\psi_\beta/kT)$ from (3) and (4) and by replacing $[Na^+]$ and $[Cl^-]$ with the electrolyte bulk concentration C

$$K'_- = \frac{[SiO^-]}{[SiO^- - Na^+]} C \exp (-q\psi_\beta/kT) \qquad (7)$$

$$K'_+ = \frac{[SiOH_2^+]}{[SiOH_2^+ - Cl^-]} C \exp (q\psi_\beta/kT). \qquad (8)$$
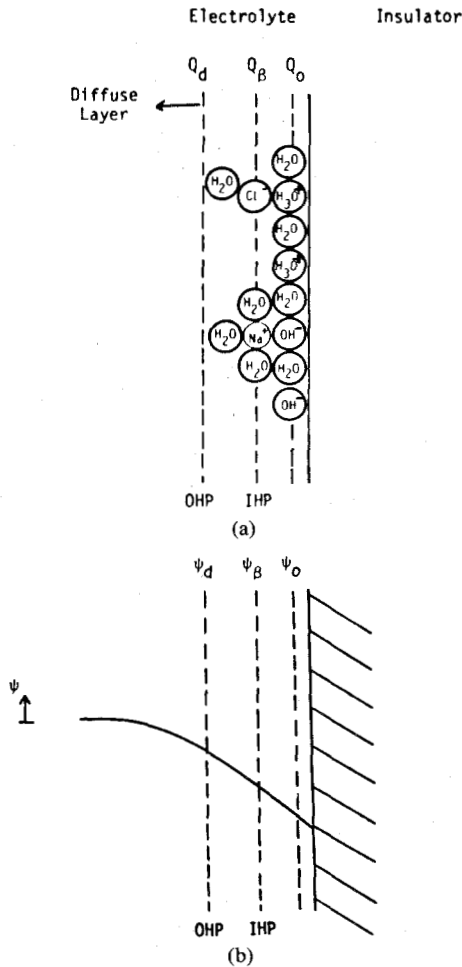
Fig. 1. Schematic diagram showing (a) the charge distribution and (b) potential profile at the insulator–electrolyte interface with surface charged sites.

The fractions of the surface sites are introduced by defining

$$\theta'_+ = [SiOH_2^+ - Cl^-] \, n_{av}/AN_S$$

$$\theta'_- = [SiO^- - Na^+] \, n_{av}/AN_S$$

$$\theta_0 = [SiOH] \, n_{av}/AN_S$$

$$\theta_+^0 = [SiOH_2^+] \, n_{av}/AN_S$$

$$\theta_-^0 = [SiO^-] \, n_{av}/AN_S$$

where n_{av} is Avogadro's number (number per mole), A is the surface area available in solution (square centimeters per liter) [18], [SiOH] and similar bracketed surface species are the equivalent concentration of surface species in moles per liter, and N_s is the total number of available sites. Therefore

$$\theta_0 + \theta_-^0 + \theta'_- + \theta_+^0 + \theta'_+ = 1. \tag{9}$$

With the fractions defined above, from (5) and (6)

$$-2.303 \, \Delta pH = q\psi_0/kT + 1/2 \ln (\theta_+^0/\theta_-^0) \tag{10}$$

where $\Delta pH = pH - pH_{pzc}$, and pH_{pzc} is defined by $pH_{pzc} = -1/2 \log (K_+ K_-)$. One can see from (1) and (2) that pH_{pzc} corresponds to the pH at the point of zero charge on the surface, i.e., $[SiOH^+] = [SiO^-]$.

Also from (5) and (6)

$$K_-/K_+ = \theta_+^0 \theta_-^0 /\theta_0^2. \tag{11}$$

Equations (7) and (8) can be rewritten as

$$\frac{C}{K'_-} \exp (-q\psi_\beta/kT) = \frac{\theta'_-}{\theta_-^0} \tag{12}$$

$$\frac{C}{K'_+} \exp (q\psi_\beta/kT) = \frac{\theta'_+}{\theta_+^0}. \tag{13}$$

Up to this point, equations have been established for the compact layer of the electrified interface. The remainder of the electrified interface, the diffuse layer which extends from the OHP to the bulk of the electrolyte, can be described by the Gouy–Chapman theory [16], [18], which is based on the Poisson and Boltzmann equations. The diffuse layer charge Q_d in a column of unit cross-sectional area extending from the boundary of the diffuse layer to the bulk of the electrolyte is related to the mean potential ψ_d at the OHP as

$$Q_d = -(8\epsilon\epsilon_0 nkT)^{1/2} \sinh (q\psi_d/2kT) \tag{14}$$

where ϵ is the dielectric constant of the solution, ϵ_0 is the permittivity of free space, and n is the bulk number density of the electrolyte ions.

By knowing the double-layer structure at the insulator–electrolyte interface, it is possible to consider the EIS system as a whole. First, the theory regarding the charge and potential distributions in an ideal EIS structure will be formulated with the following assumptions:

1) In the electrolyte the ionic concentration is sufficiently low that the Boltzmann distribution law for ions applies. Therefore, the diffuse part of the electrical double layer at the insulator–electrolyte interface can be described by the Gouy–Chapman theory.

2) At the surface of the insulator, hydroxyl groups exist which can be ionized by the hydrogen ions or hydroxyl ions to produce charged sites, which subsequently form complexation with the supporting electrolyte ions.

3) The bulk of the insulator is perfect in the sense that there is no transport of charge carriers or uncharged species.

4) There are neither charges within the insulator nor surface state charges at the semiconductor–insulator interface. Interface states at the semiconductor–insulator interface are also neglected.

5) The semiconductor is nondegenerate, and therefore the Boltzmann distribution for the charge carriers is applicable.

Several commonly used insulator films, such as silicon dioxide, aluminum oxide, silicon oxynitride, and silicate glass, contain Si–O–Si or Al–O–Al structures which produce surface hydroxyl groups upon hydrolyzing in the electrolyte solution. Assumption 2 may be extended to ac-
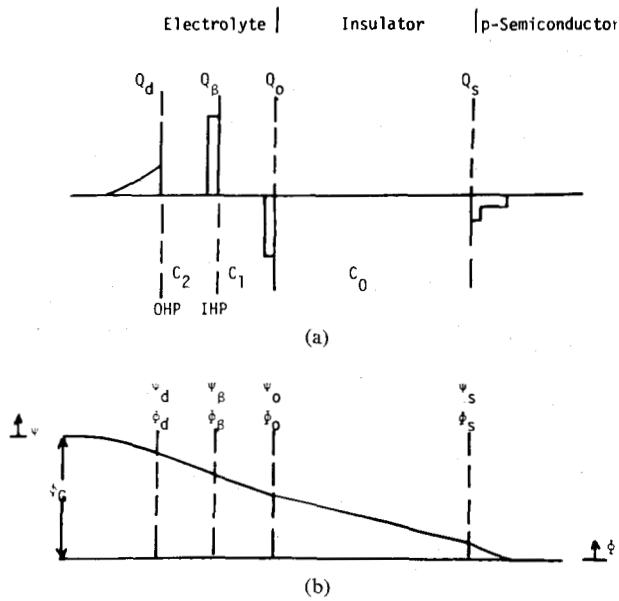
Fig. 2. (a) Charge and (b) potential distributions in an ideal electrolyte–insulator–semiconductor structure.

count for other interactions that might occur at a specific electrolyte–insulator interface.

The justification for assumption 3 relies critically on the properties of the insulator films. Because of variations in the fabrication processes, it is quite possible that imperfect insulator films will result; therefore, the transport of charge carriers or uncharged species may occur during immersion in aqueous solutions. This situation will be discussed later.

In assumption 4, for simplicity, charges within the insulator or at the semiconductor–insulator interface are not considered. In practical situations, these charges exist and are process-dependent. As in standard MOS theory [19], these charges can be taken into account by a flat-band voltage. This effect will be included in the derivation of the theoretical model of the EISFET in a later section.

Fig. 2 shows the charge and potential distribution of an ideal EIS structure with a p-type semiconductor substrate. In Fig. 2, the charge at the surface of the insulator Q_0 is shown to be negative, which is the case for $pH > pH_{pzc}$. The p-type semiconductor is shown to have an inversion layer at the surface. For convenience in later derivation of the EISFET theory, the potentials in Fig. 2 are designated by two sets of notations. The potentials ψ_d, ψ_β, ψ_0, and ψ_s are the electrostatic potentials at the OHP, the IHP, the insulator surface, and the semiconductor surface, respectively, in reference to the electrolyte bulk potential; likewise, the potentials denoted by ϕ's are the corresponding potentials with respect to the semiconductor bulk potential.

The potential difference ϕ_G between the bulk of the electrolyte and that of the semiconductor is established through a reference electrode immersed in the electrolyte solution. Since the liquid junction potential is minimized in a reference electrode, the overall potential of the reference electrode can be treated as a constant. Therefore,

if a gate voltage V_G is applied at the reference electrode with respect to the semiconductor substrate, the potential ϕ_G will follow V_G, but deviate from it by a constant determined by the particular reference electrode in use.

Equations (9) through (13), which determine the surface interaction at an insulator–electrolyte interface, and (14), which describes the diffuse layer of the double layer, can be adapted for the ideal EIS system. The relation between the semiconductor charge Q_s and semiconductor surface potential ϕ_s is expressed [20] by

$$Q_s = \pm \frac{2\epsilon_s\epsilon_0 kT}{qL_D} \{[\exp(-u_s) + u_s + 1]$$

$$+ \frac{n_0}{p_0}[\exp(u_s) - u_s - 1]\}^{1/2} \quad (15)$$

where $u_s = q\psi_s/kT$, n_0 and p_0 are the equilibrium concentration of electrons and holes, respectively, and L_D is the extrinsic Debye length for holes defined by

$$L_D = (2kT\epsilon_s\epsilon_0/p_0q^2)^{1/2}.$$

In (15), the charge within the semiconductor Q_s, is taken as positive for $u_s < 0$, and negative for $u_s > 0$.

The charge neutrality of the system requires that

$$Q_s + Q_0 + Q_\beta + Q_d = 0 \quad (16)$$

and the charges and potentials at the interfaces are related by the following equations.

$$\psi_0 - \psi_\beta = (Q_0 + Q_s)/C_1 \quad (17)$$

$$\psi_\beta - \psi_d = -Q_d/C_2 \quad (18)$$

$$\psi_\sigma - \psi_0 = Q_s/C_0 \quad (19)$$

where C_1 and C_2 are the unit-area capacitances of the inner and outer parts of the compact layer, respectively, and C_0 is the unit-area capacitance of the insulator film.

The system of equations that describe an ideal EIS system can be summarized as follows. Equations (9) through (14) represent the reaction at the electrolyte-insulator interface and the charge potential relationship in the electrolyte diffuse layer, whereas equation (15) describes the charge potential relation on the semiconductor surface. The requirement of charge neutrality is expressed by (16). The link between the different regions of the system is contained in (17) through (19). In an EIS system, the semiconductor surface charge Q_s plays a role in determining the interfacial properties, as indicated by (17) and (19). On the other hand, measurement of Q_s at the semiconductor surface provides a means of obtaining the surface potential ψ_0 at the electrolyte–insulator interface.

In a later derivation for the current–voltage characteristics of an EISFET, a strong inversion approximation [19] at the semiconductor surface will be employed. This approximation assumes that, once the semiconductor surface is strongly inverted, the surface potential will remain constant at a value approximated by $\phi_s = 2\phi_F$, where ϕ_F is the Fermi potential of the semiconductor. The approxi-
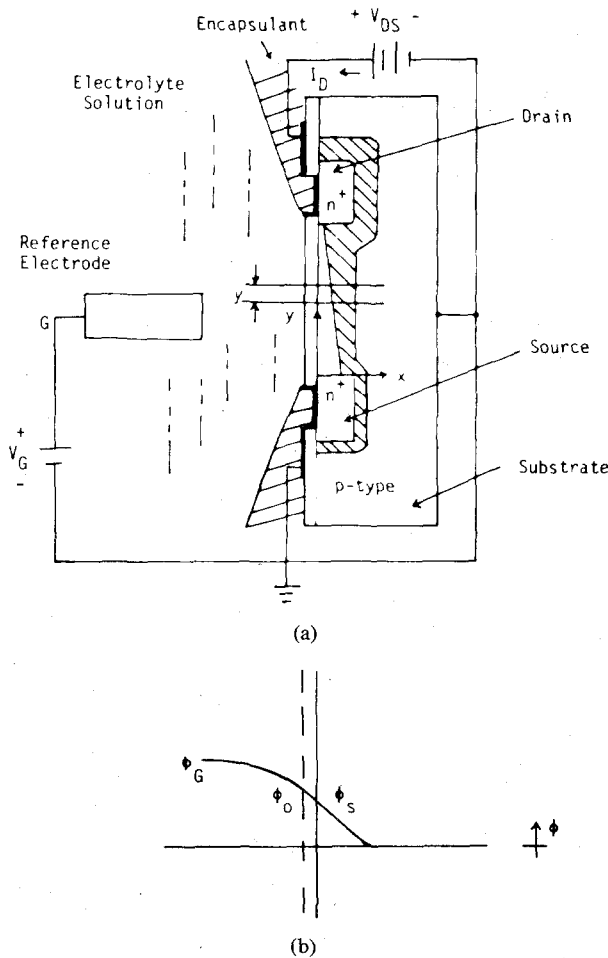
(a)

(b)

Fig. 3. (a) Cross-sectional view and (b) potential distribution of an EIS-FET.

mation of strong inversion, when it is written in terms of ψ_s, can then be expressed as $\phi_G \cong -\psi_S + 2\phi_F$.

B. Drain Current–Voltage Characteristics of an EISFET

In this section, first the current–voltage characteristics of the EISFET in an electrolyte solution are derived; then the EISFET response to electrolyte solutions under the condition of a constant drain current and drain voltage is formulated.

Consider the n-channel EISFET with the source connected to the substrate at a ground potential as shown in Fig. 3. Because of the close association (1 to 1.5 Å) of the adsorbed ions in the IHP with the charged sites on the insulator surface [18], the lateral field in the y direction due to the applied drain voltage is negligible compared to the normal field in the x direction at the inner zone of the double layer. The estimated value of the latter is three orders of magnitude higher than the value of the former. Therefore, it is reasonable to assume that the lateral field, due to the drain-to-source voltage, will not affect the insulator surface potential ϕ_0. This has also been substantiated by an experimental investigation [21] which shows no detectable effect of the lateral fringe field on the response of the EISFET. Therefore, the insulator potential

ϕ_0 will be taken as a constant value along the direction of the channel and is independent of the location y.

The potential ϕ_0 is related to the semiconductor surface charge and potential by

$$\phi_0 - \phi_{0(FB)} = -\frac{Q_s(y)}{C_0} + \phi_s(y)$$

where $\phi_{0(FB)}$ is the flat-band potential defined as the value of ϕ_0 to achieve the flat-band condition within the semiconductor, i.e., $\phi_{0(FB)} = Q_{SS}/C_0$, where Q_{SS} is the effective surface state charge. This flat-band potential represents the effect of charges due to surface states at the semiconductor-insulator interface, as well as the charges within the insulator. It is assumed that the flat-band potential $\phi_{0(FB)}$ is a parameter that depends on the fabrication process, but is not influenced by the surface field at the semiconductor nor by the interaction occurring at the insulator-electrolyte interface.

Following the standard deviation for the drain current-voltage characteristics of MOSFET [19], with the gate voltage replaced by the insulator surface potential ϕ_0, one can obtain the drain current-voltage characteristics of an EISFET in the nonsaturation region as

$$I_D = \frac{W}{L} \mu_n^* C_0 \left\{ [\phi_0 - \phi_{0(FB)} - 2\phi_F - V_{DS}/2] V_{DS} \right.$$
$$\left. -\frac{2}{3} \frac{\sqrt{2\epsilon_s\epsilon_0 qN_A}}{C_0} [V_{DS} + 2\phi_F]^{3/2} - (2\phi_F)^{3/2}] \right\} \quad (20)$$

where L is the channel length, W is the channel width, and μ_n^* is the effective electron mobility. In the saturation region, as the conduction channel is pinched off, the drain current can be approximated by a constant value which is the drain current at the pinchoff voltage.

For practical purposes the characteristics can be approximated by (21) and (22).

Nonsaturation region:

$$I_D = \beta[(\phi_0 - \phi_T)V_{DS} - (V_{DS})^2/2] \quad (21)$$

Saturation region:

$$I_D = \frac{\beta}{2}(\phi_0 - \phi_T)^2 \quad (22)$$

where $\phi_T = (Q_{SS}/C_0) + 2\phi_F - (Q_B/C_0)$; β is a constant and Q_B is the charge in the depletion region of the semiconductor.

It should be reemphasized that the above derivation of the drain current-voltage characteristics is based on the surface potential ϕ_0 at the insulator. The threshold voltage ϕ_T is a quantity determined by the semiconductor substrate, the insulator capacitance, and the fabrication process which gives rise to the $\phi_{0(FB)}$ term. Since the threshold voltage of a MOSFET is

$$V_T = \phi_{MS} + \frac{Q_{SS}}{C_0} + 2\phi_F - \frac{Q_B}{C_0}$$

therefore

$$V_T = \phi_T + \phi_{MS}$$

where ϕ_{MS} is the work function difference between the metal and the semiconductor. It is possible to estimate the value of ϕ_T by measuring the threshold voltage of a monitor MOSFET on the same chip. While by definition ϕ_T is not associated with the behavior at the electrolyte–insulator interface, the EISFET does respond to the electrolyte solution through the term ϕ_0.

In the operation of an EISFET, a common method is to bias the device at a constant drain current and drain voltage. This is achieved by using a feedback circuit which varies the gate voltage to restore the drain current as the electrolyte parameters are changed. Therefore, the gate voltage measured in such a feedback circuit provides information about the electrolyte solution.

Working in either the nonsaturation or the saturation region when the EISFET is biased at a constant drain current and voltage, the surface potential ϕ_0 of the gate insulator is fixed according to the drain current–voltage characteristics. Since the electrolyte bulk potential ϕ_G only deviates from the gate voltage V_G by a constant value determined by the particular type of reference electrode used, the problem of finding the response of the EISFET in terms of the gate voltage becomes a situation of solving the EIS system to obtain ϕ_G as a function of the electrolyte condition.

At first glance, solving ϕ_G to find the response of the EISFET in electrolyte solutions appears to be a two-dimensional problem. A closer examination of the EIS interfaces in Fig. 3 reveals that, although the surface potential ϕ_S of the semiconductor varies along the channel and the substrate caused by the voltage drop due to the drain current, the potential in the electrolyte is only a function of the x axis, with $\phi = \phi_0$ at the insulator surface and $\phi = \phi_G$ in the electrolyte bulk. Therefore, to solve for ϕ_G, one can choose any plane of a constant y coordinate between the source ($y = 0$) and the drain ($y = L$). Nevertheless, it is advantageous to select the plane at $y = 0$ because the semiconductor surface potential ϕ_S at that point is maintained at its equilibrium value of $2\phi_F$ due to the absence of reverse bias between the channel and the substrate.

Therefore, to find the response of EISFET's in electrolyte solutions operated at a constant drain current and drain voltage, the procedure is first to calculate the potential ϕ_0, determined by the drain current–voltage characteristics, (21) or (22). The set of simultaneous equations for the EIS system using the strong inversion approximation is then solved for ϕ_G, assuming a constant ϕ_0 determined from the drain current–voltage characteristics. This approach has been taken to arrive at theoretical calculations which are then compared with experimental results described in the next section.

III. EXPERIMENTAL METHODS AND RESULTS

The structure and geometry of the EISFET's used in the experiments have been reported elsewhere [7]. The
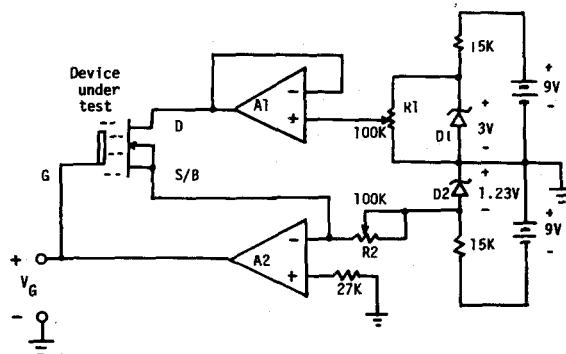

Fig. 4. Schematic diagram of the measurement circuit.

EISFET's were n-channel depletion-mode FET's built on p-type (100) silicon substrates with a resistivity of 10 Ω · cm. A thermally grown layer of 880-Å silicon dioxide served as the gate insulator. The channel length is 20 μm with a large channel width-to-length ratio of approximately 90 : 1 achieved by an interdigitated configuration. The diffused drain and source regions are extended to one end of the chip to facilitate lead attachment and packaging.

The EISFET's, which used a calomel reference electrode as the gate, were connected to a measurement circuit with a digital voltmeter to provide output readings. The experiments were carried out at a room temperature of 23°C. During titration measurement, the pH value was monitored by a pH meter (Orion 901). The schematic diagram of the measurement circuit is shown in Fig. 4. The circuit allows the drain voltage and drain current to be set individually by $R1$ and $R2$, respectively. The operational amplifier $A2$ provides a feedback so that the gate voltage V_G is varied during the titration measurement. In this way the drain current of the EISFET is maintained at a constant value set by the variable resistor $R2$. The gate voltage V_G serves as the output in response to electrolyte solutions being tested. The drain voltage was set at 3 V and the drain current at 100 μA to 1 mA. As far as the relative output voltage is concerned, no difference was observed within experimental error for different drain currents.

Simple 1 : 1 valent electrolyte solutions, including KCl, NaCl, and LiCl, were used. These solutions did not contain any buffer substances and were titrated with the appropriate hydroxides (e.g., NaOH for NaCl solutions) and hydrochloric acid solutions.

The devices were tested in a standard pH 7 buffer solution, both before and after titration experiments, to provide calibration points for the devices. All the devices responded to titrations within several seconds. However, they exhibited a long-term drift of 5 to 10 mV/h and a hysteresis on the order of 10 mV.

Typical experimental results for the silicon dioxide EISFET's in NaCl solutions are shown in Fig. 5 indicated by data points. For low concentrations (10^{-5} M), titration was only carried out toward the acidic side to avoid adding NaOH, which could alter the cation ion concentration of the solutions at high pH value. In this low concentration
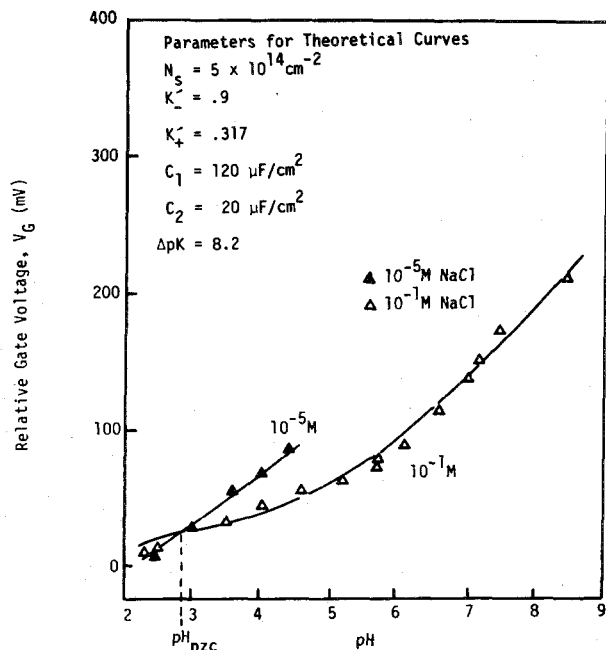
Fig. 5. Experimental result of silicon dioxide EISFET by titration.

Fig. 6. Comparison of the effect between Li^+, K^+, and Na^+ ions on the silicon dioxide EISFET.

solution, addition of hydrochloric acid can alter the anion concentration; however, as long as the device is in the range of $pH > pH_{pzc}$, the anions will not affect the device's response. The response for the 10^{-5} M concentration is rather linear and much steeper than that for the 10^{-1} M. The latter is flattened in the lower pH range, where there is a predominance of the electrolyte ions on the diffuse layer, but it turns steeper in the higher pH range due to the enhancement of the surface ionization by the electrolyte ions in forming complexes with the charged sites.

In Fig. 5, the solid lines indicate the results of theoretical calculation. The constants N_s, C_1, C_2, K'_+, and K'_- were chosen based on the work of Davis et al. [18], Abendroth [22], and Dugger et al. [23]. The ΔpK value was adjusted to fit the experimental data. ($\Delta pK = pK_- - pK_+$.) It was found that $\Delta pK = 8.2$ provided a good fit of the theoretical calculations and the experimental results. The ΔpK value is in good agreement with the value of 8.4 given by Davis et al. In order to match the theoretical curves with the experimental data, the point of $\Delta pH = 0$ occurs at 2.8 in the pH axis. This value of $pH_{pzc} = 2.8$ is consistent with the published values [24] of 1.5 to 3.0 for silicon dioxide.

A comparison of the effects between the lithium, sodium, and potassium ions is shown in Fig. 6. Data points for an NaCl solution are reproduced from Fig. 5. The theoretical curves indicate a 6-mV difference at $\Delta pH = 6$ between KCl and LiCl solutions. Since the reproducibility of the silicon dioxide EISFET is limited to approximately 10 mV due to hysteresis and slow drift, it is not possible to distinguish the difference between the solutions as shown in the figure.

IV. DISCUSSION

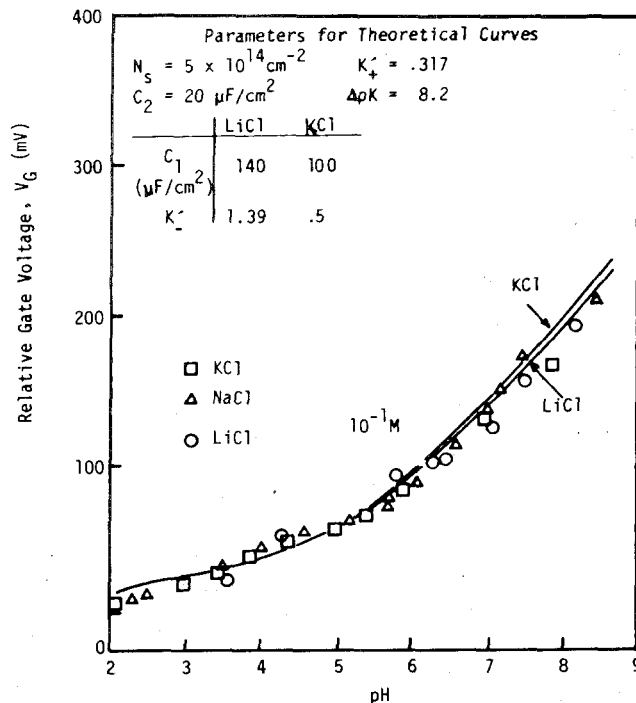It is apparent that good correlation between the experimental results and the theoretical calculations was ob-

served. It should be emphasized that the relative response of the EISFET's is independent of the operation point, provided the drain current is reasonably low so that the variation of the semiconductor charge ΔQ_s due to varied drain current is negligible compared to the total insulator surface charge ΔQ_0. For the operating drain current from 1 μA to 1 mA, the response is found to be essentially independent of the operating current. Only minor differences on the order of a few millivolts appear at $\Delta pH = 0$ for very low electrolyte concentrations, e.g., 10^{-5} M. Under constant current with feedback, variation of the device's electrical parameters, such as β, ϕ_T, and ϕ_F, will cause a variation of ϕ_0. In effect, these parameters will vary the operating point but do not play a role as far as the relative response of the EISFET's is concerned. However, the electrochemical parameters of the insulator–electrolyte interface are significant in determining the performance of the EISFET as a pH sensor.

The pertinent electrochemical parameters of the insulator–electrolyte interfaces can be obtained from electrochemical measurement of the interfacial properties. Although the data on this subject are rather limited, some are available for certain oxide–electrolyte interfaces. The main purpose of the following sections is to discuss the effect of these electrochemical parameters on the behavior of EISFET's in response to the electrolyte pH values and ionic concentrations. Among these parameters, the ratio of the surface ionization constants, K_-/K_+, is of particular importance. To facilitate discussions of the response of EISFET's, a constant ΔpK is defined as $\Delta pK = pK_- - pK_+$ or $\Delta pK = -\log(K_-/K_+)$. Typical values for the electrochemical parameters are taken from the literature [16], [18].
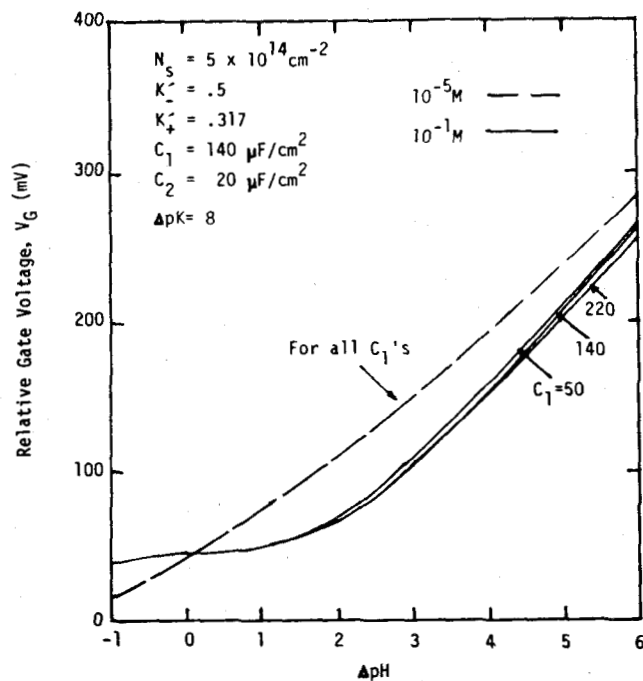
Fig. 7. The effect of the inner layer capacitance C_1 on the response of an EISFET.

Fig. 8. The effect of surface complexation constant K'_- on the response of an EISFET.

A. The Compact Zone Capacitances

Both Yates *et al.* [16] and Davis *et al.* [18] agreed to use 20 μF/cm^2 for the outer layer capacitance C_2 of the compact zone for the electrical double layer. This is a reasonable value to adopt from the classical value of the compact layer capacitance of Hg and AgI [25], [26]. Therefore, the same value of C_2 is used in the present study. However, there is some disagreement about the values of the inner-layer capacitance C_1 based on how close the adsorbed ion species can reach the surface of the insulator. Yates *et al.* [16] use a constant inner-layer capacitance C_1 of 140 μF/cm^2 for all oxides and electrolytes, while Davis *et al.* [18] claim 140 μF/cm^2 is an appropriate value for lithium ions, but a smaller value, i.e., 100 to 125 μF/cm^2, should be used for potassium ions because they are larger than the lithium ions. To a certain degree, through the effect of complexation, the inner-layer capacitance C_2 will affect the charges at the insulator; however, it was found that the EISFET's response is very insensitive to the variation of C_1's in a wide range as shown in Fig. 7. In this figure, C_1 varies from 50 to 220 μF/cm^2, and the response for the EISFET is plotted for electrolyte concentrations of 10^{-5} and 10^{-1} M. For electrolyte concentrations of 10^{-5} M, the curves for the relative EISFET gate voltages at different C_1's overlap each other due to the lack of surface complexation for low electrolyte concentrations. For the higher electrolyte concentrations of 10^{-1} M, although minor differences do appear at higher ΔpH because of surface complexation, only a variation of approximately 10 mV is obtained at ΔpH = 6 between C_1 = 50 and 220 μF/cm^2. There is essentially no difference between the curves as ΔpH approaches zero.
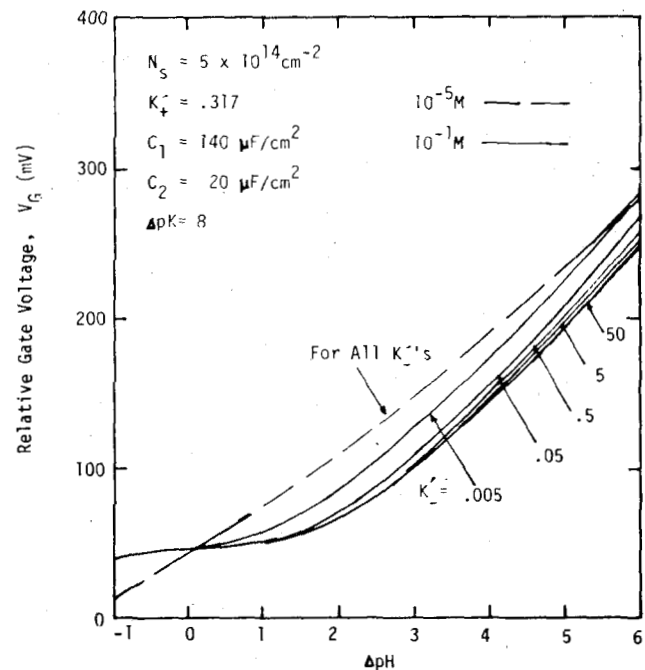
The above discussions, based on Fig. 7, are for a high ΔpK value of 8. For lower ΔpK values, the EISFET's response is expected to be even less sensitive to the variation of C_1's because of the less important role of surface complexation at lower ΔpK values.

B. Surface Complexation Constants

Other than the inner layer capacitance C_1, the effect that various supporting electrolyte ions have on each other is mainly determined by the surface complexation constants, i.e., K'_- and K'_+. The K'_+ value, which determines the adsorption of anions to form complexes with positive sites, is found to have essentially no effect on the device's response in the region of ΔpH > 0, possibly due to the lack of positively charged sites.

On the other hand, the K'_- value, which determines the adsorption of cations to form complexes with negatively charged sites, has a certain effect on the response for high electrolyte concentrations in the region of ΔpH > 0. In Fig. 8 it is shown that, with decreasing K' values, the response for 10^{-1} M moves toward the response for 10^{-5} M.

While the inner-layer capacitance C_1 is related to the distance between the adsorbed charge plan (IHP) and the surface charge plane, the surface complexation constants K'_+ and K'_- indicate the tendency of the ions to form complexes with the charged sites. One can recall from (9) and (10) the smaller the K'_+ and K'_- values, the stronger the tendency for surface complexation. As shown by Fig. 8 in the region of ΔpH > 0, as K'_- decreases the flattened portion of the 10^{-1} M EISFET response at low ΔpH tends to become steeper and the 10^{-5} M curve moves toward the 10^{-5} M curve. This effect may be attributed to a higher
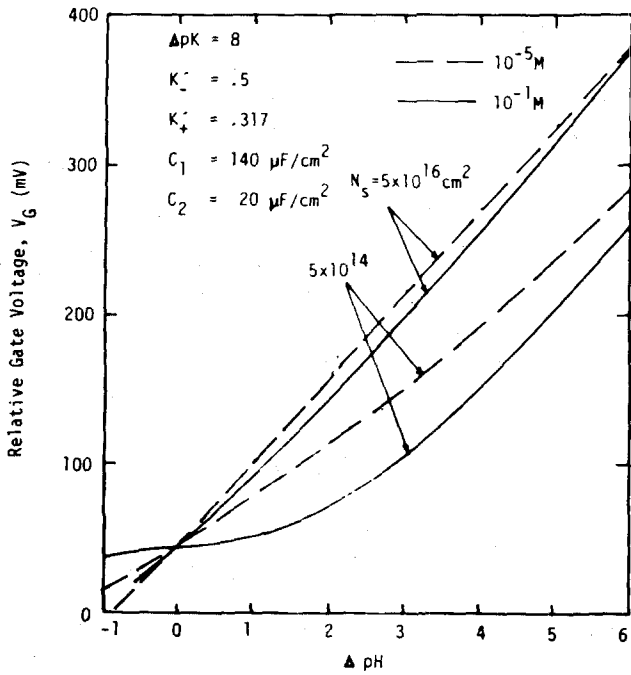
Fig. 9. The effect of the number of surface sites N_s on the response of an EISFET.
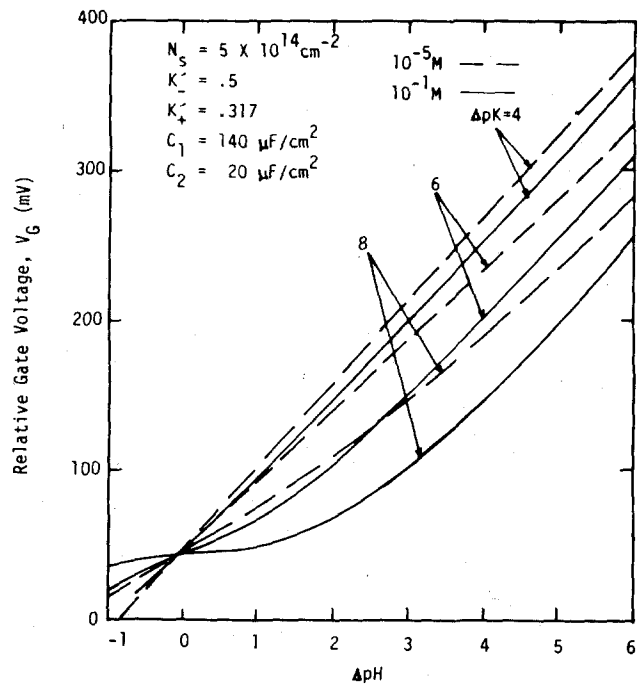

Fig. 10. Effect of the separation of the surface ionization constant ΔpK on the reponse of an EISFET.

degree of surface complexation which enhances the surface ionization.

The above discussions have been on the positive side of the ΔpH axis; a similar conclusion can be drawn for the negative side of the ΔpH axis with the roles of K'_- and K'_+ interchanged.

C. Surface Site Density

The total surface site density N_s is also a factor of interest due to its important property of providing available sites for surface interaction. As can be seen from Fig. 9, a large N_s results in higher pH sensitivity and smaller interference effect for the electrolyte ions over the hydrogen ions in terms of a steeper curve and smaller separation between the 10^{-5} and the 10^{-1} M curves. However, unless N_s is extraordinarily high, in the normal range of 10^{14} to 10^{15} cm^{-2}, the effectiveness of ionizing the sites also has to be considered.

D. Surface Ionization Constants

The separation of the surface ionization constants ΔpK is a parameter of paramount importance in determining the response of EISFET's in terms of application as a pH sensor. To illustrate the general trends regarding the effect of ΔpK on the response of EISFET's, Fig. 10 shows the response of EISFET's as a function of ΔpH for different ΔpK values at electrolyte concentrations of 10^{-5} and 10^{-1} M. As shown in Fig. 10, a lower ΔpK results in higher p H sensitivity and smaller interference effect for the electrolyte ions over the hydrogen ions.

For more quantitative comparisons, two quantities are defined as shown in the insert in Fig. 11. The first quantity is the slope m, defined by the difference of the relative gate
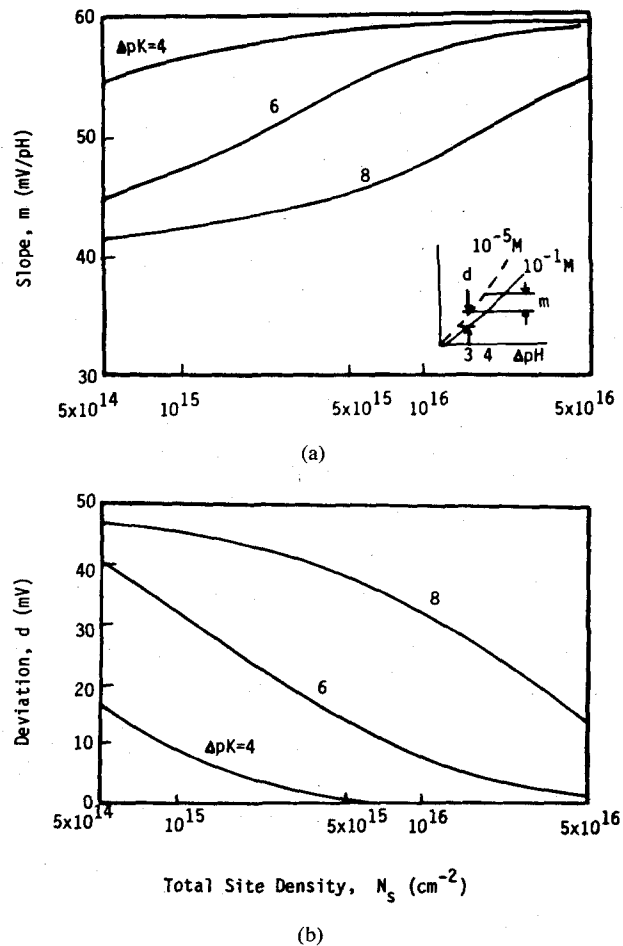

(a)

(b)

Fig. 11. Effect of N_s and ΔpK on the p H performance of an EISFET. (a) Slope versus density, (b) deviation versus density.

TABLE I
ELECTROCHEMICAL PARAMETERS OF TWO OXIDE-ELECTROLYTE SYSTEMS

SYSTEM	POINT OF ZERO CHARGE pH_{pzc}	SURFACE SITE DENSITY $N_s (10^{14} cm^{-2})$	IONIZATION CONSTANTS		
			pK_+	pK_-	ΔpK
Al_2O_3/NaCl [27],[28]	8.5	8 [29]	7.68-7.9	9.1	1.2
SiO_2/KCl [18],[22]	1 - 3	4.6 - 5 [30]	-1.2	7.2	8.4

voltage between $\Delta pH = 4$ and 3 for the electrolyte concentration of 10^{-5} M. The slope m is expressed in millivolts per pH and represents the pH sensitivity of the device. The second quantity is the deviation d, defined by the difference of the relative gate voltage between electrolyte concentrations of 10^{-5} and 10^{-1} M at $\Delta pH = 3$. The deviation is expressed in millivolts and represents the interference effect of the device as a pH sensor.

The slope m and the deviation d are plotted in Fig. 11(a) and (b), respectively, as functions of N_s with different ΔpK values. Generally speaking, as in the case for most of the oxides studied, N_s varies over a relatively narrow range from 5×10^{14} to 1.2×10^{15} cm^{-2} [18], whereas ΔpK can vary in a large range from 1.2 to 8.4. Therefore, for normal insulator surfaces, it is expected that the dominant factor in determining the pH performance of the EISFET is the ΔpK value. This is true unless certain surface modification methods are available that drastically increase the number of surface sites enormously to enhance the pH performance regardless of the ΔpK value.

In summary, the EISFET is a device that measures the phenomena occurring at the insulator-electrolyte interface. The pH sensitivity of the device arises from the ionization by hydrogen ions (H^+) or hydroxyl ions (OH^-) of the surface hydroxyl groups. These surface ionization processes are influenced by adsorbed electrolyte ions present on the charged sites to form surface complexes. The site density N_s of the surface hydroxyl groups is a factor of interest in the sense that it is the ultimate limit for the number of charged sites. Higher N_s values favor the EISFET's acting as a pH sensor. However, the separation of the surface ionization constants, expressed by a ΔpK value, is the decisive factor in determining the pH performance of the device. The response curve of the EISFET with a large ΔpK value tends to be flattened at ΔpH close to the zero, and the degree of flatness increases with electrolyte concentration. It is evident that surface hydroxyl groups with small ΔpK values are preferable for pH sensor applications.

V. CONCLUSIONS

A good correlation between the experimental results and the theoretical calculations was observed for an EISFET using silicon dioxide as the gate insulator. The generalized theory serves very well to explain the primary characteristics of an EISFET. For an EISFET to work as a pH sensor, the surface layer of the gate insulator, in the presence of an electrolyte solution, should possess a low ΔpK value.

In addition, high surface site density, N_s is preferable. Table I summarizes the pertinent electrochemical parameters of two oxide-electrolyte systems. It is apparent that aluminum oxide is an excellent candidate for the application of the EISFET as a pH sensor due to the relatively large N_s and small ΔpK value. Indeed, good performance has been observed in recent literature for EISFET's using aluminum oxide [31]. The pH at zero point of charge pH_{pzc} for the different systems is also included in Table I. It is desirable to select insulator materials with a pH_{pzc} value far away from the pH range of application. However, among the three parameters, ΔpK is the prime factor in determining the performance of the EISFET when it is used as a pH sensor.

Secondary effects, such as long-term drift and hysteresis, are not considered in this theory. These phenomena can result from the slow progressive hydration of the insulator film, as well as from the transport of certain species throughout the insulator film, which affects the semiconductor-insulator interface. In a practical situation, aluminum oxide film with its passivation capability to resist hydration, as well as migration of ions or hydrogen molecules, exhibits less hysteresis and long-term drift. On the other hand, silicon dioxide film, comparatively, is much more subject to hydration and ion migrations and, therefore, results in less reproducible device performance. It is likely that the mechanism proposed by Lauks [32] suggesting a surface ion-conducting membrane on the insulator film, as well as the possible diffusion of species through the insulator film, suggested by de Rooij *et al.* [10], should be integrated with the present model to achieve a theory which can completely describe the behavior of an EISFET.

REFERENCES

[1] P. W. Cheung, D. G. Fleming, W. H. Ko, and M. R. Neuman, Eds., *Theory, Design and Biomedical Application of Solid State Chemical Sensors*. Boca Raton, FL: CRC Press, 1978.
[2] J. Janata and R. J. Huber, "Ion sensitive field effect transistors and related devices," *Ion Select. Electrode Rev.*, vol. 1, pp. 31-79, 1979.
[3] P. Bergveld, "Development of an ion-sensitive solid-state device for neurophysiological measurements," *IEEE Trans. Biomed. Eng.*, vol. BME-17, pp. 70-71, 1970.
[4] P. Bergveld, "Development, operation, and application of the ion-sensitive field-effect transistor as a tool for electrophysiology," *IEEE Trans. Biomed. Eng.*, vol. BME-19, pp. 342-351, 1972.
[5] S. D. Moss, J. Janata, and C. C. Johnson, "Potassium ion-sensitive field-effect transistor," *Anal. Chem.*, vol. 47, pp. 2238-2242, 1975.
[6] R. G. Kelly, "Microelectronic approaches to solid state ion selective electrode," *Electrochimica Acta*, vol. 22, pp. 1-8, 1977.
[7] C. D. Fung, P. W. Cheung, and W. H. Ko, "Electrolyte-insulator-semiconductor field-effect transistor," in *IEDM Tech. Dig.*, pp 689-692, 1980.

[8] M. Esashi and T. Matsuo, "Integrated micro multi ion sensor using field effect of semiconductor," *IEEE Trans. Biomed. Eng.*, vol. BME-25, pp. 184–192, 1978.

[9] S. D. Moss, C. C. Johnson, and J. Janata, "Hydrogen, calcium, and potassium ion-sensitive FET transducers: A preliminary report," *IEEE Trans. Biomed. Eng.*, vol. BME-25, pp. 49–54, 1978.

[10] N. F. deRooij and P. Bergveld, "The influence of the pH on the surface state density at the SiO_2–Si interface," in *The Physics of SiO_2 and Its Interfaces*, S. T. Patelides, Ed. New York: Pergamon, 1978, pp. 433–437.

[11] P. R. Barabash and R. S. C. Cobbold, "Dependence of interface state properties of electrolyte–SiO_2–Si Structures on pH," *IEEE Trans. Electron Devices*, vol. ED-29, pp. 102–108, 1982.

[12] A. Prolonge, P. Gentil, and G. Kamarinos, "Study of the working of ion sensitive FET," in *IEDM Tech. Dig.*, pp. 147–150, 1979.

[13] C. D. Fung, P. W. Cheung, A. S. Wong, J. A. Topich, and W. H. Ko, "Investigation of insulator materials on the response of ion-sensitive field-effect transistors (ISFET's)," in *Extended Abstracts Electrochem. Soc. Meeting*, pp. 197–199, 1978.

[14] C. D. Fung, "Characterization and theory of electrolyte–insulator–semiconductor field-effect transistor," Ph.D. dissertation, Case Western Reserve University, 1980.

[15] W. M. Siu and R. S. C. Cobbold, "Basic properties of the electrolyte–SiO_2–Si system: Physical and theoretical aspects," *IEEE Trans. Electron Devices*, vol. ED-26, pp. 1805–1815, 1979.

[16] D. E. Yates, S. Levine, and T. W. Healy, "Site-binding model of the electrical double layer at the oxide/water interface," *J. Chem. Soc. Faraday I*, vol. 70, pp. 1807–1818, 1974.

[17] L. Bousse, N. F. DeRooij, and P. Bergveld, "Operation of chemically sensitive field-effect sensors as a function of the insulator–electrolyte interface," *IEEE Trans. Electron Devices*, vol. ED-30, pp. 1263–1270, 1983.

[18] J. A. Davis, R. O. James, and J. O. Leckie, "Surface ionization and complexation at the oxide/water interface, I: Computation of electrical double layer properties in simple electrolytes," *J. Colloid Interface Sci.*, vol. 63, pp. 480–499, 1978.

[19] S. M. Sze, *Physics of Semiconductor Devices*. New York: Wiley, 1969.

[20] R. H. Kingston and S. F. Neustadter, "Calculation of the space charge, electric field and free carrier concentration at the surface of a semiconductor," *J. Appl. Phys.*, vol. 26, pp. 718–720, 1955.

[21] W. H. Ko, J. M. Lee, C. D. Fung, and P. W. Cheung, "The fringe field effect of V_{DS} on ISFET pH sensors," *Sensors and Actuators*, vol. 3, pp. 91–98, 1982/83.

[22] R. P. Abendroth, "Behavior of a pyrogenic silica in simple electrolytes," *J. Colloid Interface Sci.*, vol. 34, pp. 591–596, 1970.

[23] D. L. Dugger, J. H. Staton, B. N. Irby, B. L. McConell, W. W. Cummings, and R. W. Maatmen, "The exchange of twenty metal ions with the weakly acidic silanol group of silica gel," *J. Phys. Chem.*, vol. 68, pp. 757–760, 1964.

[24] S. M. Ahmed, "Electrical double layer at metal oxide–solution interfaces," in *Oxides and Oxide Films*, vol. 1, J. W. Diggle, Ed. New York: Marcel Dekker, 1972.

[25] W. Stumm, C. P. Huang, and S. R. Jenkins, "Specific chemical interactions affecting the stability of dispersed systems," *Croat. Chem. Acta*, vol. 42, pp. 223–224, 1970.

[26] J. Lyklema and J. T. H. G. Overbeek, "Electrochemistry of silver iodide, the capacity of the double layer at the silver iodide–water interface," *J. Colloid Sci.*, vol. 16, p. 595, 1961.

[27] H. Sadek, A. K. Hielmy, V. M. Sabet, and Th. F. Tadros, "Adsorption of potential determining ions at the aluminum oxide–aqueous interface and the point of zero charge," *J. Electroanal. Chem.*, vol. 27, pp. 257–266, 1970.

[28] C. P. Huang and W. Stumm, "Specific adsorption of cations on hydrous γ-Al_2O_3," *J. Colloid Interface Sci.*, vol. 43, pp. 409–420, 1973.

[29] J. B. Peri, "Infrared and gravimetric study of the surface hydration of Alumina," *J. Phys. Chem.*, vol. 69, pp. 211–219, 1965.

[30] C. G. Armistead, A. J. Hambleton, S. A. Mitchell, and J. A. Hockey, "The surface hydroxylation of silica," *J. Phys. Chem.*, vol. 73, pp. 3947–3953, 1969.

[31] H. Abe, M. Esashi, and T. Matsuo, "ISFET's using inorganic gate thin films," *IEEE Trans. Electron Devices*, vol. ED-26, pp. 1939–1944, 1979.

[32] I. R. Lauks, "pH measurement using polarizable electrodes," *IEEE Trans. Electron Devices*, vol. ED-26, pp. 1952–1959, 1979.

*

Clifford D. Fung (S'77–M'80) received the B.S.E.E. degree from Cheng Kung University, Taiwan, Republic of China, in 1969, the M.S. degree from Chiao Tung University, Taiwan, in 1971, and the Ph.D. degree in electrical engineering from Case Institute of Technology, Case Western Reserve University, Cleveland, OH, in 1980.

He is currently an Assistant Professor in the Department of Electrical Engineering and Applied Physics at Case. He is also an associated faculty member of the Department of Macromolecular Science. His current research interests are in the areas of silicon carbide devices, solid-state microsensors, and ploymeric thin films for electronic devices.

Dr. Fung is a member of Eta Kappa Nu and the Electrochemical Society.

*

Peter W. Cheung (S'83–M'84) received the B.S. degree in chemistry from Oregon State University, Corvallis, in 1968, the M.S. degree in chemistry from the University of Puget Sound, Tacoma, WA, in 1969, and the Ph.D. degree in electrical engineering from the University of Washington in 1973.

He was an Associate Professor at Case Western Reserve University, Cleveland, OH. He is currently a Professor of Electrical Engineering and Bioengineering at the University of Washington, Seattle. His research interests are in the areas of biomedical transducers and instrumentation for physiological research and continuous patient monitoring.

*

Wen H. Ko (S'55–M'59–SM'75–F'78) was born in China. He received the B.S.E.E. degree from the Chinese National University of Amoy in 1946 and the M.S. and Ph.D. degrees in electrical engineering from Case Institute of Technology, Case Western Reserve University, Cleveland, OH, in 1956 and 1967, respectively.

He was an Assistant and Associate Professor at Case Institute of Technology from 1954 to 1967, and has been a Professor in the Electrical Engineering Department and the Biomedical Engineering Department since 1967. Some of his areas of interest are solid-state transducers, solid-state devices and technology, and biomedical instrumentation, especially implant electronics.